Ph.D. Dissertation of Medicine

Characteristics of tonsillar and gut microbiota in IgA nephropathy and their association with clinical features

IgA 신병증에서 편도 및 장내 미생물총의 특징과 임상 양상과의 연관성

August 2021

Graduate School of Medicine
Seoul National University
Forensic Medicine Major

Ji In Park

Characteristics of tonsillar and gut microbiota in IgA nephropathy and their association with clinical features

Seong Ho Yoo

Submitting a Ph.D. Dissertation of
Medicine

April 2021

Graduate School of Medicine
Seoul National University
Forensic Medicine Major

Ji In Park

Confirming the Ph.D. Dissertation written by
Ji In Park
July 2021

Chair
Vice Chair
Examiner
Examiner
Examiner

Abstract

Background

Recent studies have revealed that alteration in microbiota has a remarkable effect on the host immune responses, particularly in autoimmune diseases. Patients with immunoglobulin A nephropathy (IgAN) commonly manifest recurrent gross hematuria with upper airway or gastrointestinal infection. Moreover, the mucosal immune system in the tonsil and gut is considered the initial site of IgAN inflammation; however, the characteristics of the tonsillar and gut microbiota in IgAN have not been fully elucidated.

Methods

To characterize the tonsillar and gut microbiota in IgAN, they were compared among three groups: IgAN, other glomerular diseases, and healthy controls. For tonsillar microbiota, 80 tonsil swab samples were obtained from patients with IgAN (n = 21), patients with other glomerular diseases (n = 36), and healthy controls (n = 23). For gut microbiota, 194 fecal samples were collected from patients with IgAN (n = 100), patients with membranous nephropathy (n = 30), and healthy controls (n = 64).

The microbiota from tonsil swabs and fecal samples was analyzed using the Illumina MiSeq system based on the 16S rRNA gene. The function of the 16s rRNA gene sequence was predicted using the Phylogenetic Investigation of Communities by Reconstruction of Unobserved States 2 (PICRUSt 2).

Results

Tonsillar bacterial diversity was higher in IgAN than in other glomerular diseases; however, it did not differ from that in the healthy controls. Moreover, principal coordinates analysis revealed differences between the tonsillar microbiota of the IgAN group and both healthy and disease controls. The proportions of *Rahnella*, *Ruminococcus*_g2, and *Clostridium*_g21 were significantly higher in patients with IgAN than in healthy controls (corrected $p < 0.05$). The relative abundances of several taxa were correlated with the estimated glomerular filtration rate, blood urea nitrogen, hemoglobin, and serum albumin levels.

Furthermore, gut bacterial diversity was similar in the three groups. The relative abundance of *Blautia* in the IgAN group was significantly higher, whereas that of *Sporobacter* was lower than that in the control or membranous nephropathy group (corrected $p < 0.01$). Using KEGG orthology analysis, 14 significantly altered

pathways were identified in the IgAN group, and the two genera significantly associated with IgAN were correlated (corrected $p < 0.05$).

Conclusion

Based on the aforementioned findings, tonsillar and gut microbiota may be associated with clinical features and immunological pathogenesis of IgAN.

Keywords: IgA nephropathy, microbiota, gut, tonsil, pathogenesis

Student Number: 2014-30599

Table of Contents

List of Tables and Figures

Tables

Figures

Chapter 1. Introduction

1.1. Study Background

Immunoglobulin A nephropathy (IgAN) is the most prevalent primary glomerulonephritis worldwide [1]. It usually affects young individuals, and a significant proportion of patients eventually progress to kidney failure [2, 3]. The prevalence and genetic risk of IgAN are higher and the kidney prognosis is worse in Asians than in other races [4, 5].

Although the etiology and pathogenesis are not fully understood, mucosal immunity has been known to be associated with the development of IgAN. Patients with IgAN frequently manifest with gross hematuria, flank pain, and acute kidney injuries simultaneously or immediately after upper respiratory or gastrointestinal illness [6] which activates mucosal immune system. Immunoglobulin A (IgA) is known to be produced mainly by the mucosal immune system [7]. Several previous findings explain and support association of the pathogenesis and mucosal immunity. For example, they could be related to serum galactose-deficient IgA1 level, which is important in the pathogenesis of the disease and is produced in mucosal tissues. The mucosal synthesis of galactose-

deficient IgA1 is known to be influenced by the innate immune system via toll-like receptors [8]. Also, on a genome-wide association study, significant loci for IgAN are associated with the maintenance of the mucosal barrier and response to mucosal pathogens [9].

The tonsil is a central site for antigen processing in the mucosal immune system and the first defensive organ against gastrointestinal entry. A common clinical manifestation of IgAN is gross hematuria, which often coincides with tonsillitis [6, 10]. As the tonsil is considered the initial site of inflammation, tonsillectomy has well-established beneficial effects in patients with IgAN suffering from recurrent tonsillitis [11, 12], either alone or in combination with steroid therapy [12-16]. Furthermore, several bacterial antigens are known to induce IgAN [17-20]. There had been two studies analyzed tonsillar microbiota in patients with IgAN as listed in Table 1. In the study published by Watanabe et al. in 2017, the tonsillar microbiota did not show any difference among IgAN, recurrent tonsillitis, and tonsillar hypertrophy [21]. However, it was based on single-center data, and urinalysis data were lacking for pediatric patients in the control group, making it impossible to exclude hidden glomerular diseases.

Additionally, the gut microbiota plays a pivotal role in

producing IgA in the intestinal mucosa in mouse models [22]. A previous review elucidated the crosstalk between the gut and kidney in IgAN, along the gut–kidney axis [23]. The gut microbial community in patients with IgAN is markedly altered compared to that in healthy controls, as summarized in Table 1 [24–29]. Moreover, previous studies presented certain gut microbiota characteristics in IgAN patients; however, the results were inconsistent due to small sample sizes ranging from 15 to 52 IgAN patients.

Table 1. List of previous studies of tonsil and gut microbiota in IgAN

Year	Sample	Country	Sample size (*n*)	Brief results
Tonsil microbiota				
2017 [21]	Tonsillar crypt	Japan	IgAN (48), Recurrent tonsillitis (21), Tonsillar hyperplasia (30)	No significant difference in microbiome composition
2020 [30]	Paraffin embedded tonsil tissue	China	IgAN (21), Chronic tonsillitis (16)	↑ *Methylocaldum* and *unclassified_f_Prevotellaceae* ↓ *Anaerosphaera*, *Halomonas*, *Trichococcus*, *Peptostreptococcus*, *norank_f_Synergistaceae* and *unclassified_k_norank_d_Bacteria*
Gut microbiota				
2014 [24]	Feces	Italy	IgAN (32) Healthy (16)	↑ *Firmicutes* ↓ *Bifidobacterium* spp.
2020 [29]	Feces	China	IgAN (17), Healthy (18)	↑ *Escherichia–Shigella*, *Hungatella, Eggerthella* ↓ *Rectale_group*
2020 [28]	Feces	China	IgAN (52), Healthy (25)	↑ *Bacteroides*, *Escherichia–Shigella*

				↓ *Bifidobacterium*, *Blautia* spp
2020 [27]	Feces	China	IgAN (44), MN (40) Healthy (30)	↑ *Escherichia−Shigella*, *Defluviitaleaceae_incertae_sedis* ↓ *Roseburia*, *Lachnospiraceae_unclassified*, *Clostridium_sensu_stricto_1*, *Fusobacterium*
2021 [26]	Feces	Malaysia	IgAN (36), Healthy (12)	↑ *Fusobacteria* phylum, ↓ *Euryarchaeota* phylum
2021 [25]	Feces	China	IgAN (15), Healthy (30)	↑ *Blautia*, *Streptococcus*, *Enterococcus* ↓ *Bacteroides*, *Faecalibacterium*

1.2. Purpose of Research

In this study, tonsillar and gut microbiota in patients with IgAN was characterized and compared with those in healthy controls, comprising live kidney donors without evidence of kidney disease, and disease controls with other glomerular diseases, in multiple centers. This study will enhance our understanding of the tonsillar and gut microbiota characteristics in IgAN patients and their association with clinical features of the disease.

Chapter 2. Body

2.1. Methods

2.1.1. Study subjects and sample collection

Patients who were admitted to undergo a kidney biopsy at three medical centers (Seoul National University Hospital, Seoul National University Boramae Medical Center, and Kangwon National University Hospital) in South Korea were enrolled. Patients were assigned to IgAN, diabetic nephropathy (DN), and membranous nephropathy (MN) groups based on the pathological evaluation. The DN and MN groups were used as disease control groups. Some of fecal samples were collected from KOrea Renal biobank NEtwoRk System TOward NExt-generation analysis (KORNERSTONE) study; multi-center, prospective cohort study and biobank for glomerular diseases [31]. All participants provided tonsil swab and fecal samples at the time of kidney biopsy, before treatment with steroids or other immunosuppressants. For tonsil analysis, subjects who visited the Seoul National Boramae Medical Center for a regular health check-up and had normal kidney function and no underlying disease served as healthy controls. For fecal analysis, kidney transplant donors who provided their feces samples at the human stool repository served as healthy controls. All subjects

were over 18 years-old, and subjects who had undergone tonsillectomy or had inflammatory bowel disease were excluded.

The demographic and clinical data for subjects were collected from hospital electronic medical records. The estimated glomerular filtration rate (eGFR) was calculated using the Chronic Kidney Disease-Epidemiology Collaboration equation [32]. Tonsil swab samples were collected by rubbing each palatine tonsil twice using a cotton swab (Easy Swab; Synergy Innovation, Seongnam, South Korea). To check a potential contamination in cotton swab, empty swabs were also analyzed along with tonsil swab samples. The samples were immediately stored at 4℃, delivered to the laboratory within 24 h, and then stored at −80 ℃ until DNA extraction.

This study was approved by the Institutional Review Board of each center (Seoul National University Hospital IRB No. 1508-046-694, Seoul National University Boramae Medical Center IRB No. 26-2015-128, Kangwon National University Hospital IRB No. KNUH-2015-07-003). The KORNERSTONE study was approved by the ethics committee of each participating center, including the institutional review boards of Seoul National University (1404-117-575), Keimyung University Dongsan Hospital (DSMC 2019-04-015-001), Chung-Ang University (1942-005-369), Severance Hospital (2019-0463-001), Boramae Medical Center (L-2019-

126), and Kangwon National University Hospital (KUNH-2019-05-009). The human stool repository included stool samples from kidney transplant donors were approved by IRB of Seoul National University Hospital (IRB number: 1703-062-839).

This study was performed in accordance with the principles of the Declaration of Helsinki. Informed written consent was obtained from each subject.

2.1.2. DNA extraction and MiSeq sequencing

Metagenomic DNA was extracted using a FastDNA SPIN Extraction Kit (MP Biomedicals, Santa Ana, CA, USA) for tonsil swab specimens and QIAamp Fast DNA Stool Mini Kit (Qiagen, Hilden, Germany) for stool samples according to the manufacturer's instructions. For MiSeq sequencing, samples were prepared as described previously [33, 34]. Briefly, the V4-5 (for tonsil) and V3-4 (for stool) variable region of the 16S rRNA gene was amplified using extracted DNA, and amplification was performed according to the protocol for preparing a 16S metagenomics sequencing library using the MiSeq system (Illumina, Inc., San Diego, CA, USA). The first step of amplification was performed in a final volume of 50 μl containing 1 μM of each primer, 2.5 U Ex Taq polymerase (Takara Bio, Otsu, Japan), 5 μl of 10 × Ex Taq buffer, 4

μl dNTP mixture, and 2 μl template DNA using a C1000 Touch thermal cycler (Bio-Rad, Hercules, CA, USA) under the following conditions: initial denaturation at 95 ℃ for 3 min; 25 cycles of denaturation at 95 ℃ for 30 s, annealing at 55 ℃ for 30 s, and extension at 72 ℃ for 30 s; and final extension at 72 ℃ for 5 min. The purification and size selection of amplicon were performed using Agencourt AMPure XP beads (Beckman Coulter, Indianapolis, IN, USA). The index PCR was performed using 5 μl of purified PCR product in a final volume of 50 μl using the Nextera XT Index Kit (Illumina) under the following conditions: initial denaturation at 95 ℃ for 3 min; 8 cycles of denaturation at 95 ℃ for 30 s, annealing at 55 ℃ for 30 s, and extension at 72 ℃ for 30 s; and final extension at 72 ℃ for 5 min. Purification and size selection were performed again using Agencourt AMPure XP Beads (Beckman Coulter). Negative controls (distilled water) were used at every step to check contamination, and the same experiments were performed for swab contamination controls. No amplicons were detected in negative controls and swab contamination controls. The quantification of library was performed using PicoGreen dsDNA Assay Kit and Qubit dsDNA HS Assay Kit (Invitrogen, Calsbad, CA, USA). Equimolar concentrations of each library were pooled and sequenced on the Illumina MiSeq System (250-bp paired-end

reads) according to the manufacturer's instructions.

2.1.3. Sequence data analysis

Tonsil swabs

Sequence reads were analysed using CLC genomics workbench v.11.0.1 with the Microbial Genomic Module (Qiagen, Aarhus, Denmark) as described previously [33, 35]. Sequence reads were merged and reads with short lengths (merged reads of <200 bp) or low-quality scores (Q < 25) and primer sequences were removed from the merged sequences using the USEARCH pipeline v.10.0.240 (http://www.drive5.com/usearch). Chimeric sequences were removed using the UPARSE tool. Resultant sequences were clustered into OTUs based on 97% identity. Taxonomic positions of representative sequences in each OTU cluster were assigned using the EzBiocloud [36]. To compare diversity indices among samples, read numbers were normalized by random subsampling and indices were calculated using MOTHUR [37]. Principal coordinates analysis (PcoA) plots were generated to compare the microbiota among samples using Calypso [38].

Fecal samples

Raw sequencing data were processed using Quantitative

Insights Into Microbial Ecology (QIIME2) microbiome analysis package [39]. The raw fastq files were converted into QIIME2 compatible files and processed them using DADA2 [40] to filter, trim, and correct low-quality reads and remove the chimeric sequences. The curated amplicon sequence variants (ASVs) were aligned and annotated using EzBiocloud [36] as the reference database. Alpha diversity was evaluated using Shannon diversity and beta diversity by Bray-Curtis distance. PCoA plots were generated to compare the microbiota among samples using R software.

2.1.4. Statistical analyses

Clinical characteristics of subjects were compared by analysis of variance (ANOVA) and chi-square tests. p-values < 0.05 were considered statistically significant. Permutation tests were used to calculate statistical significance in the PCoA. The differences in microbial taxa between samples were evaluated by the Mann–Whitney U test and Kruskal–Wallis test. The correlations between clinical features and relative abundances of specific microbes were analyzed using Spearman's rank correlation tests in SPSS (version 22). Microbial taxon abundance was compared using Multivariate Association with Linear Models (MaAsLin), adjusted for covariates

and subjected to false discovery rate (FDR) correction with q ≤ 0.05. The functional roles of microbiota were predicted using Phylogenetic Investigation of Communities by Reconstruction of Unobserved States 2 (PICRUSt2) [41]. Corrections for multiple testing were performed using the Benjamini–Hochberg method for false discovery rate adjustment. Results with corrected *p*–values of < 0.05 were considered statistically significant.

2.2. Results

2.2.1. Tonsillar microbiota

Clinical characteristics of subjects

A total of 80 subjects were included, including 21 patients with IgAN, 21 patients with MN, 15 patients with DN, and 23 healthy subjects. Clinical characteristics are summarized in Table 2. The mean age was lower in the healthy control group (32.8 ± 5.8 years) than in the disease groups (53.2 ± 14.4 years, $p < 0.001$). Hypertension was more prevalent in all disease groups than in healthy controls ($p < 0.001$). The levels of plasma hemoglobin, serum albumin, and serum calcium were lower in IgAN group than in healthy controls ($p < 0.001$). Patients with MN showed features of nephrotic syndrome, including hypercholesterolemia, hypoalbuminemia, and large amounts of proteinuria. Kidney function,

as evaluated by eGFR, was lowest in DN, followed by IgAN. Proteinuria and hematuria were common in the disease controls and IgAN groups.

Table 2. Baseline characteristics of subjects included in analysis of tonsillar microbiota

	Healthy control (n = 23)	IgA nephropathy (n = 21)	Membranous nephropathy (n = 21)	Diabetic nephropathy (n = 15)	p-value
Age (years)	32.8 ± 5.8	47.8 ± 18.1	56.2 ± 11.0	56.5 ± 11.0	<0.001
Male [n (%)]	15 (65.2)	11 (52.4)	13 (61.9)	12 (80.0)	0.401
Body mass index (kg/m^2)	24.2 ± 4.1	25.1 ± 2.7	26.2 ± 5.9	25.6 ± 4.1	0.498
SBP (mmHg)	119.8 ± 14.9	127.8 ± 20.4	128.7 ± 17.0	134.4 ± 25.9	0.142
DBP (mmHg)	80.7 ± 12.5	81.1 ± 16.2	79.3 ± 11.7	78.9 ± 16.1	0.961
Smoking [n (%)]	4(17.4)	7 (33.3)	3 (14.3)	1 (7.1)	0.219
Hypertension [n (%)]	0 (0.0)	11 (52.4)	9 (42.9)	10 (66.7)	<0.001
Diabetes mellitus [n (%)]	0 (0.0)	4 (19.0)	2 (9.5)	15 (100.0)	<0.001
Hemoglobin (g/dL)	15.0 ± 1.6	13.0 ± 2.5	12.6 ± 1.7	10.4 ± 1.6	<0.001
Glucose (mg/dL)	92.1 ± 9.1	117.7 ± 35.8	113.4 ± 24.2	135.5 ± 95.0	0.047
Total cholesterol (mg/dL)	196.3 ± 39.8	205.4 ± 77.9	249.1 ± 81.0	177.9 ± 45.4	0.009
Albumin (g/dL)	4.4 ± 0.2	3.5 ± 0.8	2.8 ± 0.7	3.5 ± 0.7	<0.001
Calcium (mg/dL)	9.2 ± 0.4	8.6 ± 0.8	8.2 ± 0.6	8.6 ± 0.6	<0.001
Phosphorus (mg/dL)	3.4 ± 0.2	3.6 ± 0.8	3.6 ± 0.5	3.8 ± 0.9	0.238
Uric acid (mg/dL)	5.7 ± 1.6	6.4 ± 1.7	6.2 ± 1.8	7.3 ± 2.9	0.116

Blood urea nitrogen (mg/dL)	11.1 ± 2.6	23.5 ± 19.1	14.8 ± 3.5	31.0 ± 15.3	<0.001
Creatinine (mg/dL)	0.9 ± 0.1	1.7 ± 1.8	0.8 ± 0.2	2.2 ± 1.7	0.001
eGFR (mL/min/1.73 m^2)	107.7 ± 12.8	69.0 ± 37.4	92.0 ± 15.6	45.6 ± 23.8	<0.001
Proteinuria [*n* (%)]					<0.001
negative~trace	23 (100.0)	3 (14.3)	0 (0.0)	1 (7.1)	
1+~2+	0 (0.0)	4 (19.0)	2 (9.5)	3 (21.4)	
3+~4+	0 (0.0)	14 (66.7)	19 (90.5)	10 (71.4)	
Hematuria [*n* (%)]					<0.001
<1/HPF	13 (56.5)	0 (0.0)	1 (4.8)	4 (29.6)	
1~4/HPF	10 (43.5)	3 (14.3)	8 (38.1)	6 (42.9)	
>5/HPF	0 (0.0)	18 (85.7)	12 (57.1)	4 (28.6)	
Urine protein to creatinine ratio (mg/mg)	–	3.7 ± 2.9	6.2 ± 3.8	5.9 ± 4.7	0.081

SBP; systolic blood pressure, DBP; diastolic blood pressure, eGFR; estimated glomerular filtration rate, HPF; high-power field. Data are presented as mean ± standard deviation or number (percentage); the *p*-value for comparison of all four groups

Diversity and phylum composition of the tonsillar microbiota

A total of 3,443,894 sequence reads (average 43,048.7 reads per sample) were obtained from 80 tonsil swabs. Although the mean age differed significantly among groups (Table 2), there were no significant differences in bacterial diversity according to age in each group ($p > 0.05$; Fig. 1). As shown in Figure 2, I detected more operational taxonomic units (OTUs) in the IgAN and healthy control groups than in the MN and DN groups ($p < 0.01$). The compositions

of the microbiota differed among groups in a PcoA based on Bray–Curtis distances ($p < 0.01$ by permutation tests; Fig. 2C). The microbiota of MN was more similar to that of DN than to those of the IgAN and healthy control groups. Individual variation was higher in the IgAN group than in the other groups. *Firmicutes*, *Proteobacteria*, *Bacteroidetes*, and *Actinobacteria* were the dominant phyla in all groups (Fig. 2D). The relative abundance of *Proteobacteria* (55.7% of the total microbiota) was higher in the healthy control than in the other groups (33.8% to 40.8%), whereas the proportions of *Firmicutes* and *Bacteroidetes* were higher in all disease groups than in healthy control groups. Although the average proportions of each phylum differed among groups, these differences were not statistically significant (corrected $p > 0.05$).

Figure 1. Bacterial diversity of tonsillar microbiota according to age within each group.

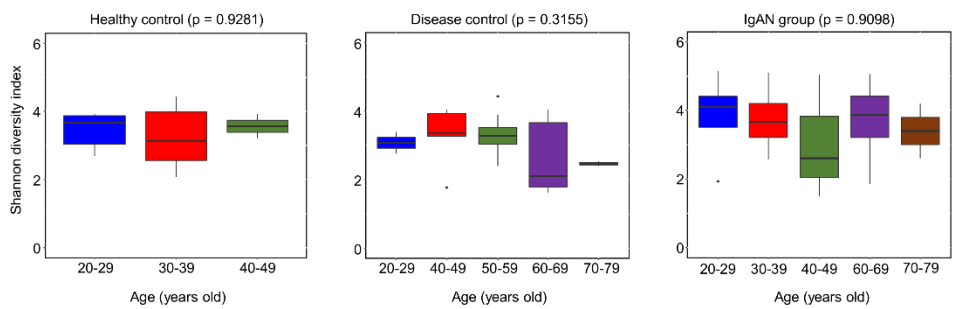

Figure 2. Comparison of diversity and phylum composition of the tonsillar microbiota among groups. (A) OTU counts were compared after the normalisation of the read number for each sample. (B) Shannon diversity indices were compared. (C) The principal coordinated analysis plot of tonsillar microbiota based on Bray–Curtis distances. Significance was estimated by permutation tests. (D) Comparison of the phylum composition among groups. Relative abundance is expressed as the mean value for each group. Comparisons were performed using Mann–Whitney U tests. (**p < 0.01). OTUs, operational taxonomic units.

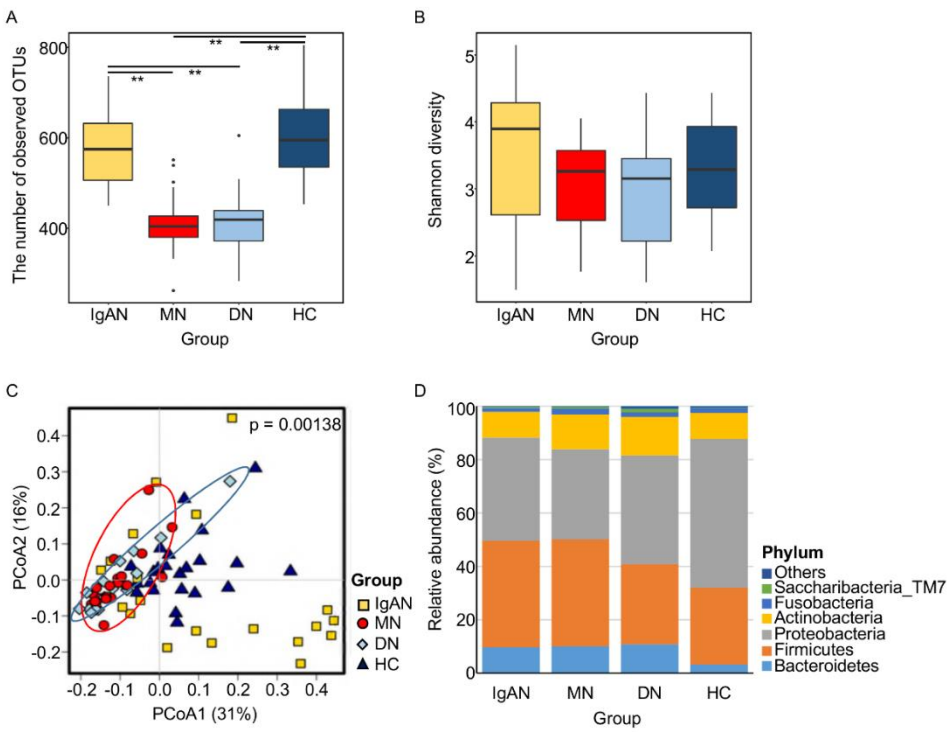

Significantly different microbes among groups

To detect significantly different genera, frequently detected genera were compared among groups (Fig. 3). Frequently detected genera were defined as genera that comprised >0.5% (mean value) of the microbiota in more than 50% of the samples in each group. *Streptococcus*, *Pseudomonas*, *Neisseria*, and *Haemophilus* were the dominant genera (>5% in each group) in all groups. The relative abundances of *Rahnella*, *Ruminococcus_g2*, and *Clostridium_g21* were significantly higher in the IgAN group than in the healthy control group (corrected $p < 0.05$; Fig. 4). More genera differed between the MN and healthy control (17 genera) or IgAN groups (14 genera) than between the DN and healthy control (10 genera) or IgAN groups (1 genus) (corrected $p < 0.05$). *Tannerella*, *Eubacterium_g10*, *Faecalibacterium*, *Lachnoanaerobaculum*, uncultured *Veillonellaceae*, *Citrobacter*, *Acinetobacter*, and uncultured *Moraxellaceae* were commonly different between the healthy control and MN or DN groups. Conversely, there were no common genera between the IgAN and MN or DN groups.

Figure 3. Composition of genera in the tonsillar microbiota from all samples.

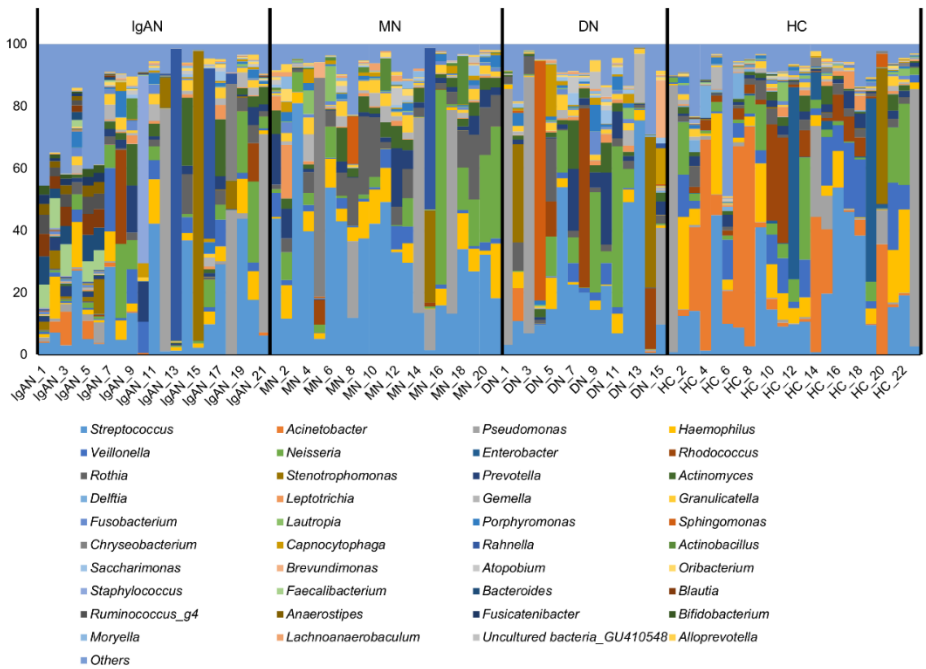

Figure 4. Genera with significant differences in abundance between patients with IgAN and the healthy control group. Significance was evaluated by Mann–Whitney tests and corrected by the Benjamini–Hochberg method (**corrected $p < 0.01$, *corrected $p < 0.05$).

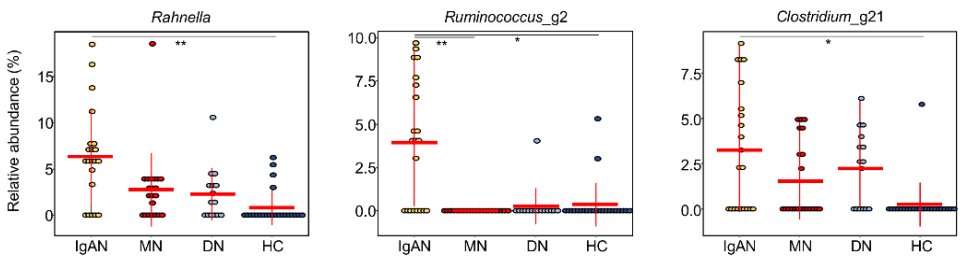

Correlation between genera and clinical features

I analysed the correlations between the relative abundances of genera and clinical features using Spearman's rank correlation coefficients with corrected p-values. Four genera having significantly different abundance between the IgAN and healthy control were also correlated with clinical features (corrected $p < 0.05$). The relative abundances of two genera, *Acinetobacter* and uncultured *Moraxellaceae*, were correlated with kidney function represented by eGFR and blood urea nitrogen (BUN) (Fig. 5). They were positively correlated with eGFR values and negatively correlated with BUN values. In addition, *Acinetobacter*, uncultured *Moraxellaceae*, and *Enterobacter* were positively correlated with plasma hemoglobin values (Fig. 6). *Acinetobacter*, uncultured *Moraxellaceae*, and *Delftia* were positively correlated with serum albumin values (Fig. 6). Three genera with significant differences in abundance between the healthy control or IgAN and disease control groups were correlated with eGFR, albumin, BUN, and hemoglobin values (Fig. 7). *Tannerella* was negatively correlated with eGFR values, and *Citrobacter* was positively correlated with albumin values. *Capnocytophaga* was positively correlated with BUN values but negatively correlated with hemoglobin values.

Figure 5. Correlations between the tonsillar microbiota and clinical features in all participants. Correlations of *Acinetobacter* and uncultured *Moraxellaceae* with eGFR and BUN were evaluated by corrected *p*-values. eGFR, estimated glomerular filtration rate; BUN, blood urea nitrogen.

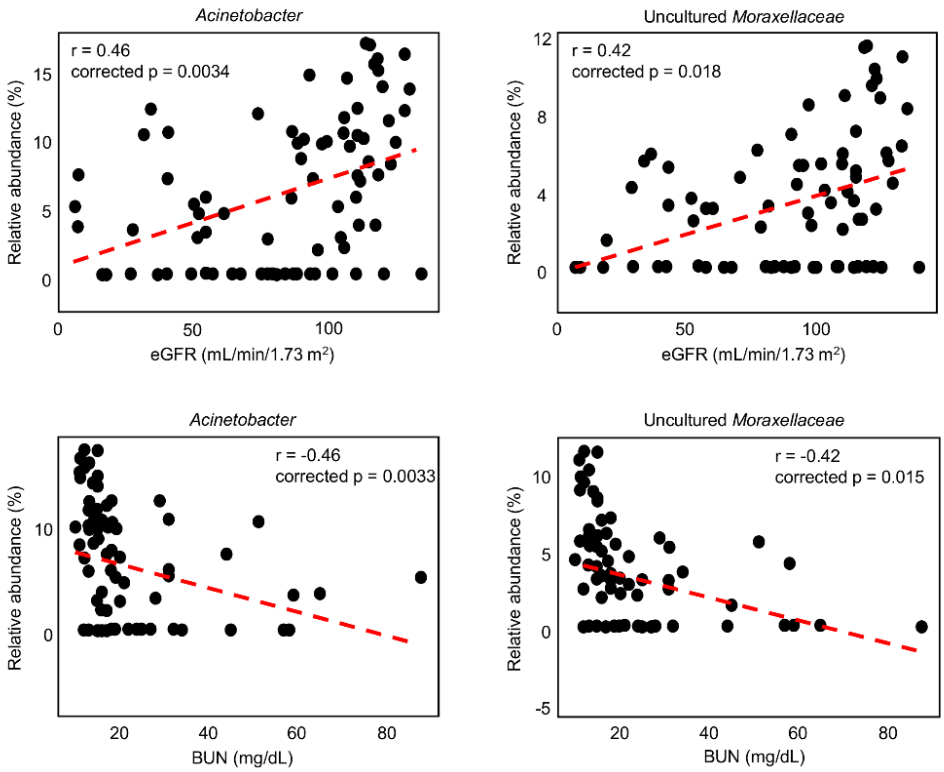

Figure 6. Correlations between tonsillar microbes and clinical features. Genera differed significantly between patients with IgAN and healthy controls. The correlations were selected by corrected *p*-values.

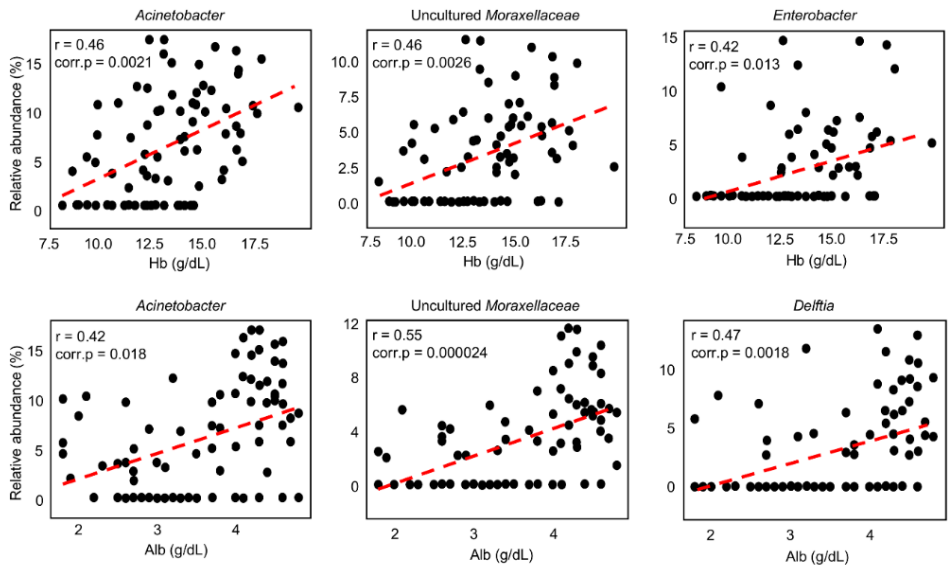

Figure 7. Correlations between tonsillar microbes and clinical features. Genera were significantly different between healthy controls or patients with IgAN and other kidney diseases. The correlations were evaluated by corrected p-values.

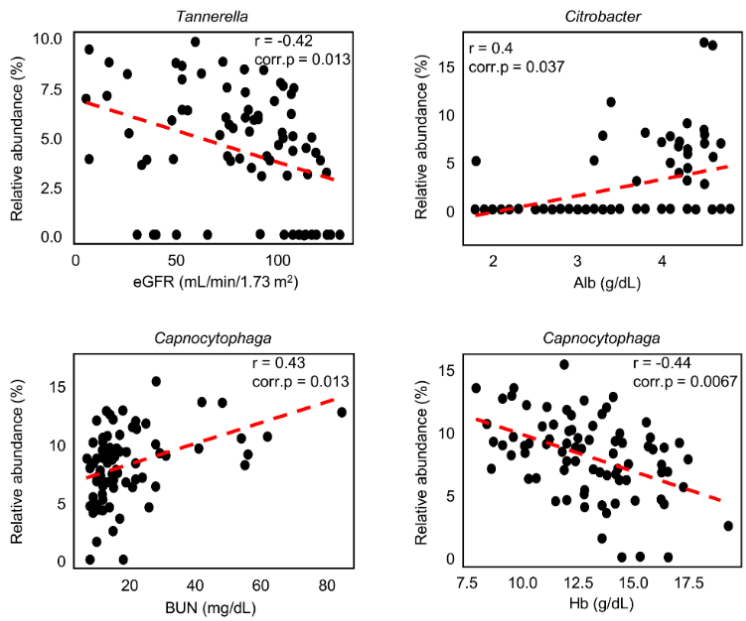

2.2.2. Gut microbiota

Clinical characteristics of subjects

A total of 194 fecal samples were analyzed from 100 patients with IgAN, 30 patients with MN, and 64 healthy subjects. Clinical characteristics are summarized in Table 3. The mean age was significantly higher in the MN group (56.1 ± 9.4 years) than in the healthy and IgAN groups (48.2 ± 11.0 and 44.0 ± 15.7 years respectively, $p < 0.001$). The proportion of male sex was higher in the MN group compared to other groups ($p = 0.018$). Hypertension and diabetes were more prevalent in both the disease groups than in healthy controls ($p < 0.001$ and $p = 0.033$, respectively). The levels of plasma hemoglobin and serum albumin were higher in healthy controls than in the disease groups ($p < 0.001$). Kidney function, as evaluated by the estimated glomerular filtration rate (eGFR), was lowest in the IgAN group, followed by the MN and healthy control group. Proteinuria and hematuria were common in the IgAN and MN groups. The urine protein to creatinine ratio was highest in the MN group.

Table 3. Baseline characteristics of subjects included in analysis of gut microbiota

		Healthy control (n = 64)	IgA nephropathy (n = 100)	Membranous nephropathy (n = 30)	p-value
Age (years)		48.17 ± 11.0	44.0 ± 15.7	56.1 ± 9.4	<0.001
Male [n (%)]		23 (35.9)	50 (50.0)	20 (66.7)	0.018
Body mass index (kg/m^2)		23.8 ± 2.8	24.4 ± 3.4	25.5 ± 3.6	0.063
SBP (mmHg)		121.1 ± 12.6	126.7 ± 15.4	126.7 ± 15.8	0.045
DBP (mmHg)		76.5 ± 8.4	79.8 ± 11.7	80.2 ± 9.4	0.105
Smoking [n (%)]		10 (15.6)	17 (17.0)	6 (20.0)	0.871
Hypertension [n (%)]		9 (14.1)	42 (42.0)	15 (50.0)	<0.001
Diabetes mellitus [n (%)]		0 (0.0)	10 (10.0)	2 (6.7)	0.033
Hemoglobin (g/dL)		13.7 ± 1.3	12.4 ± 2.6	12.9 ± 1.4	<0.001
Glucose (mg/dL)		102.6 ± 13.8	106.1 ± 25.3	112.3 ± 28.8	0.160
Albumin (g/dL)		4.3 ± 0.3	3.9 ± 0.6	2.7 ± 0.6	<0.001
Calcium (mg/dL)		9.2 ± 0.4	9.1 ± 0.6	8.2 ± 0.6	<0.001
Phosphorus (mg/dL)		3.5 ± 0.5	3.4 ± 0.6	3.7 ± 0.5	0.142
Uric acid (mg/dL)		4.8 ± 1.3	6.3 ± 1.6	6.4 ± 2.0	<0.001
Blood urea nitrogen (mg/dL)		13.1 ± 3.8	18.1 ± 10.4	16.0 ± 6.8	0.001
Creatinine (mg/dL)		0.7 ± 0.2	1.2 ± 0.8	0.9 ± 0.3	<0.001
eGFR (mL/min/1.73 m^2)		101.6 ± 15.1	82.0 ± 32.0	91.7 ± 19.9	<0.001
Proteinuria [n (%)]					<0.001
	negative~trace	54 (94.7)	8 (8.0)	0 (0.0)	
	1+~2+	3 (5.3)	56 (56.0)	5 (16.7)	
	3+~4+	0 (0.0)	36 (36.0)	25 (83.3)	
Hematuria [n (%)]					<0.001
	<1/HPF	30 (46.9)	2 (2.0)	4 (13.3)	

	1~4/HPF	32 (50.0)	15 (15.2)	6 (20.0)	
	>5/HPF	2 (3.1)	82 (82.8)	20 (66.7)	
Urine protein to creatinine ratio (mg/mg)		0.1 ± 0.0	2.1 ± 2.2	5.3 ± 3.1	<0.001

SBP; systolic blood pressure, DBP; diastolic blood pressure, eGFR; estimated glomerular filtration rate, HPF; high-power field. Data are presented as mean ± standard deviation or number (percentage); the *p*-value for comparison of all four groups

Diversity and phylum composition of the gut microbiota

A total of 18,892,806 sequence reads (average 97,385.6 reads per sample) were obtained from 194 fecal samples. Although the mean age and the sex ratio differed significantly among groups (Table 3), there were no significant differences in bacterial diversity according to age and sex ($p > 0.05$; Fig. 8). The Shannon diversity indices were calculated to evaluate differences in the ecological diversity of the microbial communities. As shown in Fig. 9A, there was no significant difference in the Shannon index among the three groups ($p > 0.05$). PCoA plots determined the similarities between microbial communities, and the result revealed no obvious difference among the groups ($p > 0.05$ by permutation tests; Fig. 9B).

Figure 8. Bacterial diversity of gut microbiota according to (A) age and (B) sex.

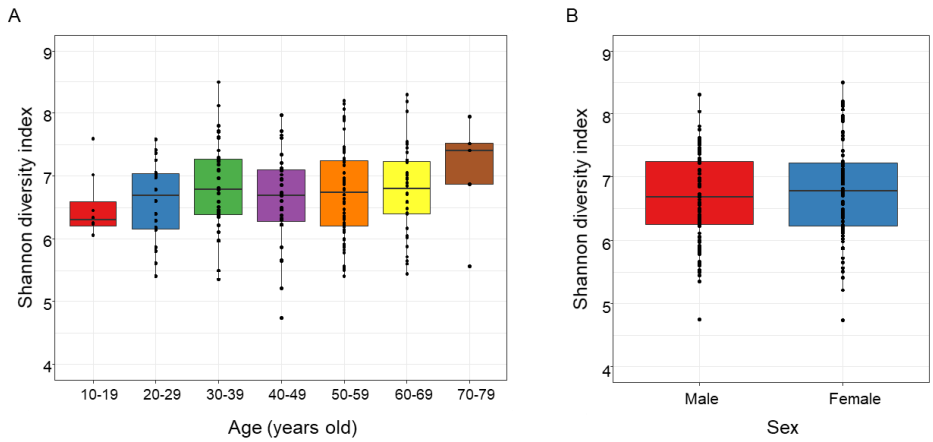

Figure 9. Comparison of the gut microbiota diversity among groups. (A) Shannon diversity indices were compared among groups. (B) The principal coordinated analysis plot of gut microbiota based on Bray–Curtis distances. Significance was estimated by permutation tests.

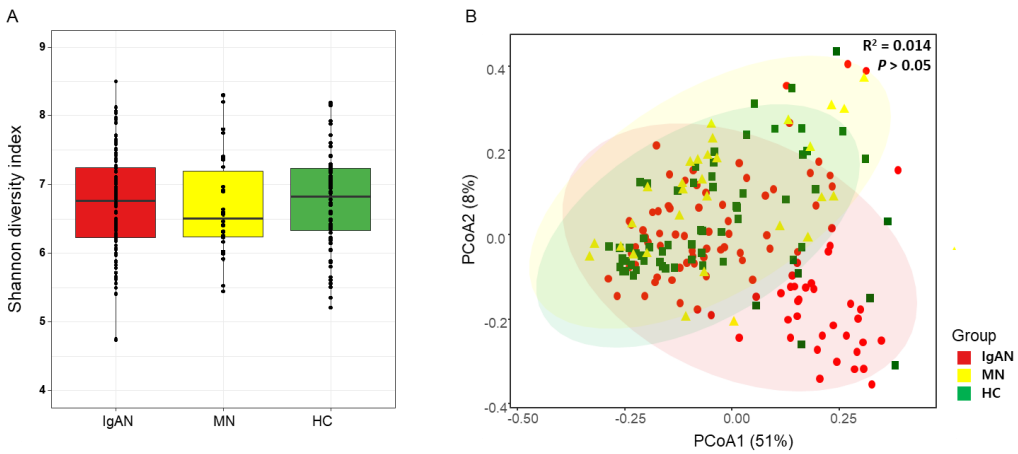

Significantly different microbes among the groups

Firmicutes, *Actinobacteria*, and *Proteobacteria* were the dominant phyla in all the groups (Fig. 10A). There was no significant difference in relative abundances among the groups at the phylum level (corrected $p > 0.05$).

To detect significantly different genera, I compared frequently detected genera among the groups (Fig. 10B). Frequently detected genera were defined as the genera comprising >1% (mean value) of the microbiota in each group. The relative abundances of *Lachnospira*, *Ruminococcus_g4,* and *Coprococcus* were significantly higher in the IgAN group than in the healthy control group (corrected $p < 0.05$; Fig. 11). The relative abundance of *Subdoligranulum* was higher in the healthy control group than in the MN group. Two genera were significantly different in the IgAN group– *Blautia* and *Sporobacter*. The relative abundance of *Blautia* was significantly higher and that of *Sporobacter* was lower in the IgAN group compared with that in the healthy control or MN group (corrected $p < 0.01$). Even after adjusting for covariates, including age and sex using MaAsLin software, abundances of *Blautia* and *Sporobacter* in the IgAN group were found to be significantly different from the other groups.

Figure 10. Comparison of the (A) phylum and (B) genus composition among groups. Relative abundance is expressed by the mean value for each group.

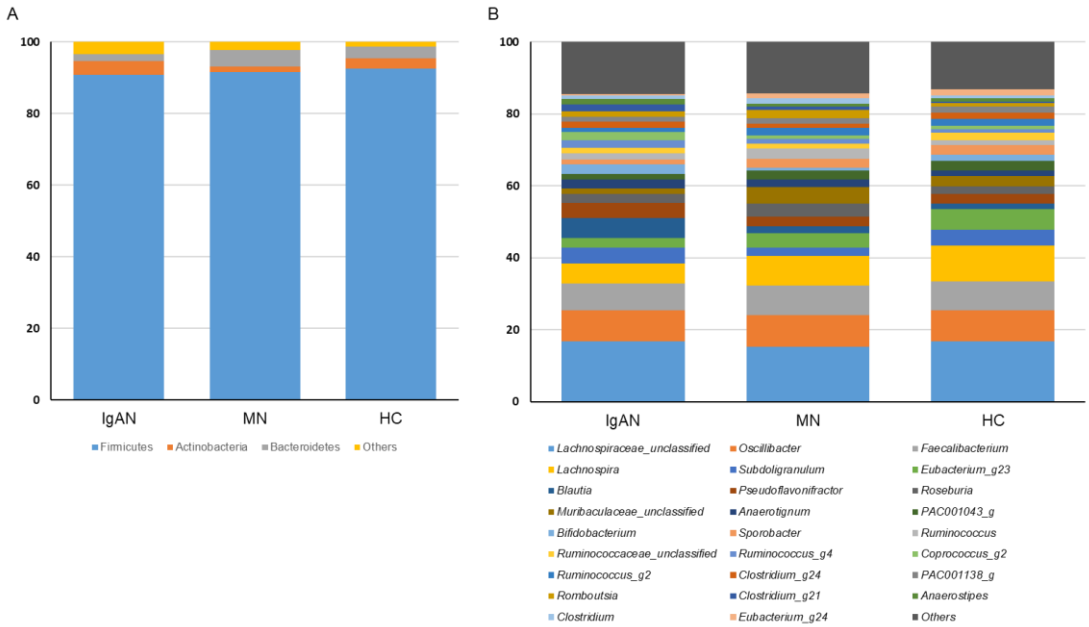

Figure 11. Genera of gut microbiota with significant differences in abundance among groups. Comparisons were performed using Mann–Whitney U tests (***$p < 0.001$, **$p < 0.01$, *$p < 0.05$).

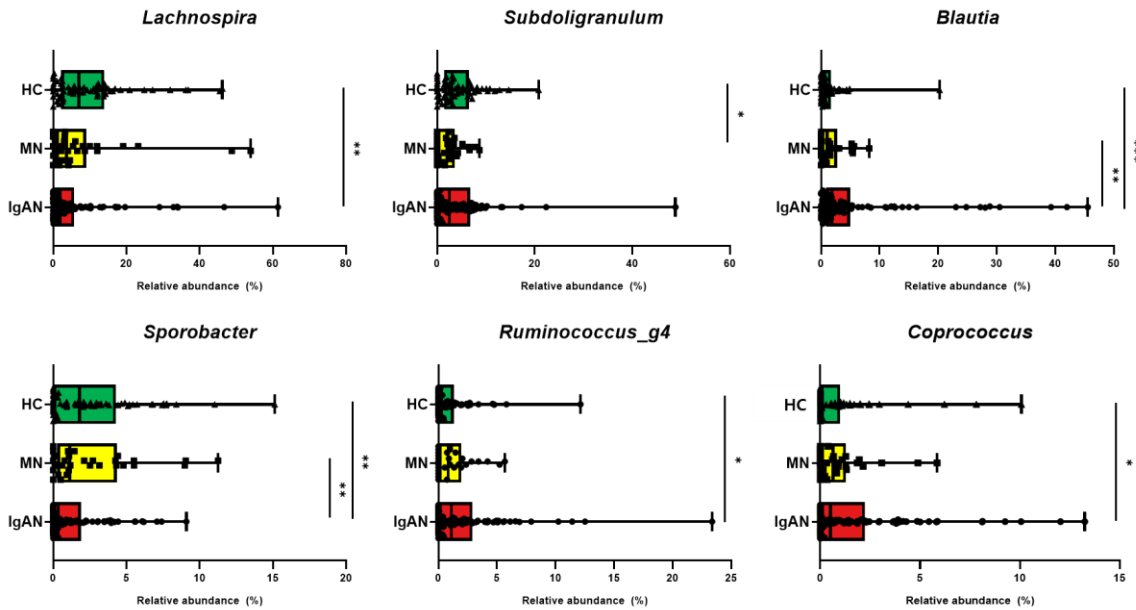

Correlation between genera and clinical features

The correlations between relative abundances of the genera and clinical features were analyzed using Spearman's rank correlation coefficients with corrected p-values. The relative abundance of *Blautia* was negatively correlated with hemoglobin level and positively correlated with BUN (corrected $p < 0.05$; Fig. 12). However, the relative abundance of *Sporobacter* did not show a significant correlation with clinical variables. It showed a marginal correlation with hemoglobin and albumin level, but it was not

statistically significant (p = 0.052 and 0.058).

Figure 12. Correlations between gut microbes and clinical features. Genera differed significantly between patients with IgAN and other groups. The correlations were selected using corrected p-values.

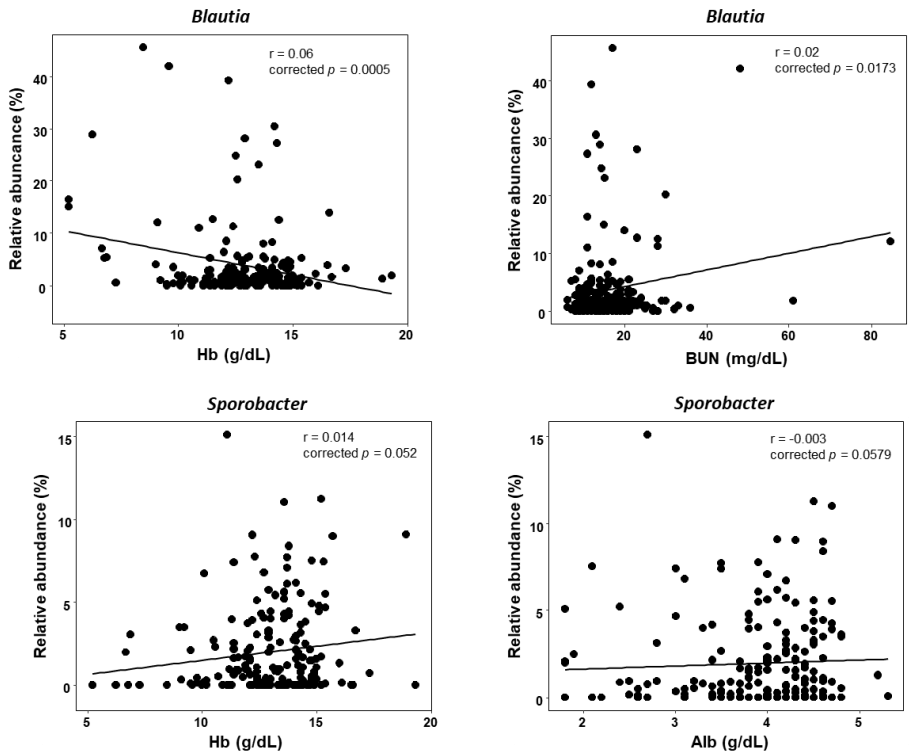

Predicted metabolic pathways associated with differential gut microbiota

PICRUSt analysis was carried out to predict metagenomic function from the 16S rRNA ASV data. Among all associated KEGG Orthology (KO) pathways determined by PICRUSt2, 47 pathways

were selected as significant in the IgAN group after adjusting for age and sex using MaAsLin (corrected $p < 0.05$). As *Blautia* and *Sporobacter* were found to be the key genera for IgAN, the pathways were narrowed down to 39 pathways, which have significant correlation with the two genera ($p < 0.05$; Fig. 13). Among them, fourteen pathways were classified as metabolic pathways, as listed in Table 4. Four pathways were negatively correlated with *Blautia* but positively with *Sporobacter*. The other ten pathways showed a positive correlation with *Blautia* but a negative one with *Sporobacter*.

Figure 13. Heatmap of the 39 significantly different KO pathways in IgAN group

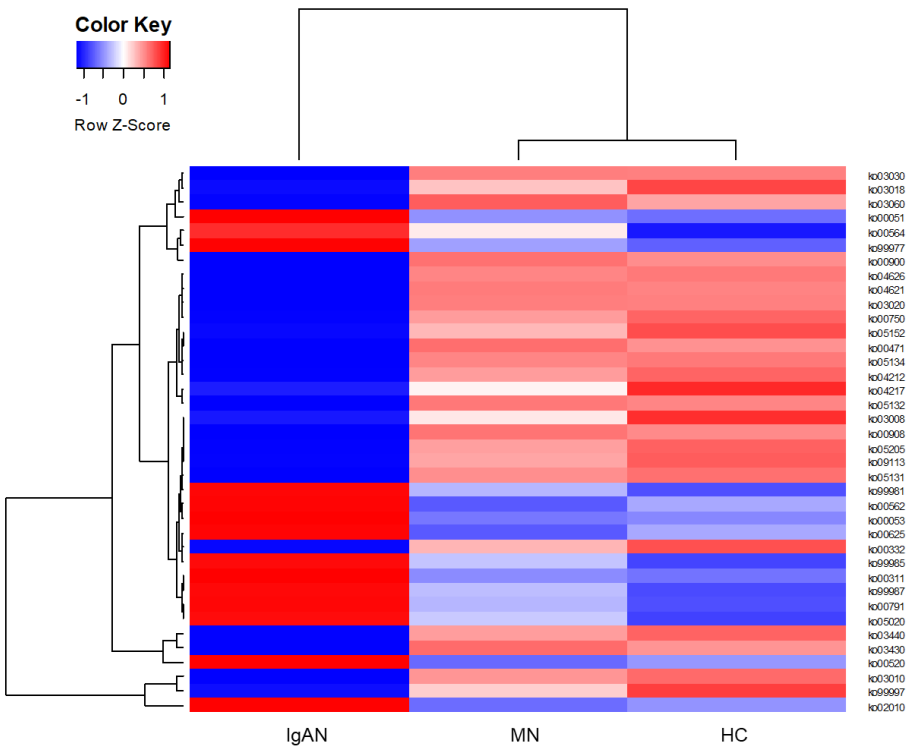

Table 4. Fourteen altered KO pathways in metabolism category

KO pathway number	Pathway name	r with *Blautia*	r with *Sporobacter*
ko00900	Terpenoid backbone biosynthesis	−0.43	0.46
ko00471	D Glutamine and D glutamate metabolism	−0.35	0.34
ko00908	Zeatin biosynthesis	−0.32	0.56
ko00750	Vitamin B6 metabolism	−0.28	0.25
ko00520	Amino sugar and nucleotide sugar metabolism	0.21	−0.40
ko00051	Fructose and mannose metabolism	0.27	−0.46

ko99981	Carbohydrate metabolism	0.27	−0.26
ko00053	Ascorbate and aldarate metabolism	0.28	−0.48
ko00564	Glycerophospholipid metabolism	0.33	−0.55
ko00625	Chloroalkane and chloroalkene degradation	0.38	−0.43
ko00562	Inositol phosphate metabolism	0.40	−0.33
ko00311	Penicillin and cephalosporin biosynthesis	0.42	−0.23
ko99985	Amino acid metabolism	0.43	−0.40
ko00791	Atrazine degradation	0.62	−0.27

KO; KEGG Orthology.

2.3. Discussion

In this study, genus−level differences in the tonsillar and gut microbiota of patients with IgAN were detected but not in patients with other kidney diseases and healthy controls [42]. *Rahnella*, *Ruminococcus_g2*, and *Clostridium_g21* were relatively abundant in the tonsils of patients with IgAN. The relative abundance of *Blautia* was significantly higher, whereas that of *Sporobacter* was lower in the gut of patients with IgAN than that of controls. Fourteen KEGG Orthology pathways differed significantly in the IgAN group compared to controls as well as correlated with abundances of *Blautia* and *Sporobacter*. Moreover, the tonsillar and gut microbiota was related to the clinical features, particularly kidney function.

The dominant phyla obtained in the tonsil samples were *Proteobacteria*, *Firmicutes*, *Actinobacteria*, and *Bacteroidetes*, which was consistent with previous findings (Fig. 2) [43].

Furthermore, bacterial richness was higher in the IgAN and healthy control groups than in the MN and DN groups. In previous studies, *Haemophilus parainfluenzae* and *Staphylococcus aureus* have been identified as candidates for introducing IgAN [17–20]. Moreover, *Treponema* and *Campylobacter* are also associated with the development and progression of IgAN [44]. Furthermore, *Prevotella*, *Porphyromonas*, and *Treponema* are highly abundant in patients with IgAN than in patients with tonsillar hyperplasia [21]. In the present study, *Haemophilus* was the dominant genus in all groups; *Staphylococcus*, *Treponema*, and *Campylobacter* were also detected in all groups (Fig. 3), but the differences in relative abundances were not significant. Furthermore, it was found that the relative abundances of *Rahnella*, *Ruminococcus_g2*, and *Clostridium_g21* were significantly higher in IgAN than in the healthy controls (corrected $p < 0.05$; Fig. 4). These inconsistencies with previous studies have several potential explanations, including differences in the sampling sites, methods for detecting bacteria, and geographic region. For sampling sites, differences have been observed in the microbiota composition between the tonsil surface and tissues [45]. In the present study, tonsil swabs were used; however, a previous study used surgically obtained tonsillar crypt tissue [21]. Most previous studies reported *in vitro* experiments revealing the effect

of specific bacterial antigens on lymphocytes in patients with IgAN; however, these methods did not detect bacteria. In contrast, in the present study, a high-throughput sequencing approach was used, which provided a comprehensive overview of the bacterial microbiota. Eventually, differences between the results of the present study and those of a previous study using a high-throughput sequencing approach [21] could be explained by different method in sample collection as explained above and different geographic region, as both affect the human microbiota [46, 47].

Three bacteria were highly abundant in the tonsil in the IgAN group than in the healthy control group. *Rahnella* sp. has been isolated from blood, surgical wounds, urine, sputum, bronchial washings, tonsils, and stool [48]. This bacterium can cause bacteremia from a kidney focus [49] and infection in immunosuppressed individuals [50]. *Ruminococcus_g2* and *Clostridium_g21* were evaluated via hierarchical clustering analysis of reference sequences in the EzTaxon-e database (https://www.ezbiocloud.net/) based on 16S rRNA genes. *Ruminococcus_g2* belongs to a cluster including *Ruminococcus bromii* and uncultured *Ruminococcus*. *R. bromii* has been detected in the microbiota of adenoiditis and tonsillitis [51] as well as in the

intestine of patients with HIV-1 infection [52]. *Clostridium_g21* belongs to a cluster including *Clostridium scindens* and uncultured *Clostridium*. *C. scindens* can covert glucocorticoids into androgens [53] and is involved in resistance to *C. difficile* infection [54]. These three bacteria related to tonsillitis are particularly abundant in the tonsils of patients with IgAN; hence, they are considered novel candidates for the pathogenesis of IgAN or for related differences in the immune system status.

The genera with significant differences with respect to relative abundance between the MN and DN groups were not detected. Moreover, higher number of differences were observed in genera between the healthy control and MN (17 genera) or DN groups (10) than between the healthy control and IgAN groups (6). Furthermore, the differences observed in the tonsillar microbiota among kidney diseases could be associated with the pathogenesis or progression of each disease. In particular, remarkable differences were observed between MN and healthy control or IgAN groups than between DN and the healthy control or IgAN groups. The development of DN involves chronic systemic inflammation, whereas primary MN is an autoimmune disease mainly mediated by antibodies to podocyte antigens, M-type phospholipase A2 receptor, and thrombospondin type 1 domain-containing 7A [55]. The tonsil

has immunological functions, and thus, the tonsillar microbiota may be more closely related to pathogenesis of MN than to the pathogenesis of DN. Differentially abundant genera in the tonsillar microbiota of each kidney disease may be used as potential candidates for further functional studies.

The correlations between the relative abundances of genera and clinical features of kidney functions were assessed (Figs. 5 and 6). Anemia is a well-known clinical feature of acute kidney injury or chronic kidney disease [56, 57]. Hypoalbuminemia is common in advanced chronic kidney disease, including end-stage kidney disease [58], and is associated with high mortality in acute kidney injury and chronic kidney disease [59]. In the present study, *Acinetobacter* and uncultured *Moraxellaceae* were related to better kidney function and higher levels of plasma hemoglobin and serum albumin in all kidney diseases. The similar patterns observed in the relationships between these parameters and specific bacteria provide a basis for further clinical studies, particularly considering the lack of research on the role of tonsillar microbiota in kidney diseases.

In addition, three genera with significant differences in relative abundance between healthy control or IgAN and disease control groups were correlated with eGFR, serum albumin, BUN, and

plasma hemoglobin (Fig. 7). *Tannerella*, found in the oral cavity and tonsilloliths, is associated with the production of volatile sulfur compounds and periodontitis [60, 61], which is linked to chronic kidney disease [62]. The correlation between a high abundance of *Tannerella* and decreased kidney function (as evaluated by eGFR) might be related to periodontitis caused by this pathogen. *Capnocytophaga* is majorly found in the oral cavity and palatine tonsil of HIV-infected individuals [63]. *Capnocytophaga ochracea* produces an immunosuppressive factor and degrades immunoglobulins [64, 65]. These results highlight the potential relationship among the tonsil environment, tonsillar microbiota, and clinical features and further indicate that the tonsillar microbiota contributes to kidney diseases, including IgAN.

Several studies have characterized the gut microbiota in IgAN. Dong et al. reported that the abundances of *Escherichia–Shigella* and *Defluviitaleaceae_incertae_sedis* were significantly higher in IgAN than in the HC, whereas those of *Roseburia*, *Lachnospiraceae_unclassified*, *Clostridium_sensu_stricto_1*, and *Fusobacterium* were lower [27]. In a study performed in Malaysia, the abundance of the phylum *Fusobacteria* was significantly higher, whereas that of the phylum *Euryarchaoeota* was lower in the IgAN group [26]; however, no difference was observed between the

IgAN and HC at the genus level. Wu et al. reported that *Blautia* exhibited a remarkable upward trend in the IgAN group, whereas *Bacteroides* and *Faecalibacterium* revealed a downward trend in the IgAN group [25]. Zhong et al. reported that *Bacteroides* and *Escherichia–Shigella* levels were significantly higher in patients with IgAN than with HC, whereas the relative abundances of *Bifidobacterium* and *Blautia* were lower [28]. Four recently reported studies demonstrated inconsistent results and contradictory data for the gut microbiota in IgAN. In the present study, the relative abundance of the genus *Blautia* was higher, but that of *Sporobacter* was lower in the IgAN group compared to the HC group. Previously published results reveal that the relative abundance of *Blautia* was higher in the gut microbiota in IgAN compared to that in the HC group in one study [25] but lower in another study [28]. No previous study reported the marked presence of the genus *Sporobacter*. These inconsistencies may have presumably occurred because of the small sample sizes in previous studies and regional variation among the studies.

Blautia is a genus of anaerobic bacteria commonly present in mammalian feces and intestines [66]. It exhibits promising probiotic activity, such as an antibacterial effect; however, its relationship with various autoimmune diseases has also been reported. A higher

abundance of *Blautia* was found in the fecal microbiota of patients with irritable bowel syndrome and ulcerative colitis compared to that in healthy individuals [67, 68]. In rheumatoid arthritis patients, *Blautia* spp. and *Streptococcus* spp. were abundantly found compared to that in healthy controls [69]. In immune thrombocytopenia patients, *Blautia*, *Streptococcus*, and *Lactobacillus* were enriched, whereas *Bacteroides* were depleted [70]. *Faecalibacterium* and *Blautia* were higher in psoriasis patients compared to nonpsoriasis controls [71]. *Blautia* spp. can induce immune responses by producing cytokines such as interleukin (IL)−10, IL−8, and tumor necrosis factor (TNF)−α, which subsequently play important roles in intestinal inflammatory responses [72]. Therefore, in addition to bacterial virulence, the pathogenicity of *Blautia* is also related to autoimmune disorders. Further studies referring to these findings are needed to fully characterize and elucidate specific pathogenic mechanisms of *Blautia* spp. with respect to IgAN and its pathogenicity.

Sporobacter has not been thoroughly investigated yet. It only includes one spp., *Sporobacter termitidis*. A previous study revealed that patients with Crohn's disease, ulcerative colitis, multiple sclerosis, and rheumatoid arthritis exhibited significantly lower levels of *Gemmiger*, *Lachnospira*, and *Sporobacter* compared

with the healthy controls [73]. The abundance of *Sporobacter* has been negatively related to proinflammatory markers in an animal study [74]. This research has not evaluated the role of *Sporobacter* in IgAN in detail; therefore, further investigation is needed.

Pathway analysis revealed several metabolic pathways which are significantly different in IgAN and correlated with the abundances of *Blautia* and *Sporobacter*. Especially, there was the pathways for amino sugar and nucleotide sugar metabolism (ko00520), which includes the enzymatic conversion of UDP-N-acetyl-galactosamine (UDP-GalNAc) to UDP-N-acetyl-galactosaminuronic acid (UDP-GalNAcA). UDP-GalNAc acts as a sugar donor for mucin-type linkage (GalNAcα1-O-Ser/Thr). Underglycosylation of the IgA1 hinge region is crucial in IgAN [6]. This pattern of glycosylation mostly affects polymeric IgA1 produced in mucosal tissues, thereby indicating the involvement of gut microbiota present near the gut mucosa. Ten Hagen et al. proposed that the underglycosylation observed in IgA-mediated nephropathy may be due to the lowered expression or absence of a particular UDP-N-acetylgalactosamine:polypeptide, N-acetylgalactosaminyltransferases (ppGalNAcT, EC 2.4.1.41), necessary to complete O-glycosylation [75]. Moreover, Wyatt et al. reported that imbalance in the activities or expression of specific

glycosyltransferases in patients with IgAN accounts for increased production of galactose-deficient, O-linked glycans in the IgA1 hinge region [6]. The enzyme or the sugar donor might be a key factor in the underglycosylation of IgA1 in IgAN. Previously, a protein involved in *Pseudomonas aeruginosa* serotype O-6 LPS biosynthesis was reported to be a UDP-GalNAc dehydrogenase that catalyzes the conversion of UDP-GalNAc to UDP-GalNAcA [76]. The hypothesis is that the gut microbiota might change the balance between the sugar donor and glycosyltransferase enzymatic activity, which eventually affects IgAN pathogenesis.

This study has several limitations. First, the number of subjects included in tonsil analyses was relatively small. Considering the high variability in microbiota composition, caution is required while applying these results to the general population. Second, age and sex differences were observed among groups. Although no obvious difference was observed in the bacterial diversity according to age and sex, these parameters may affect the composition of the tonsillar and gut microbiota. Age- and sex-matched subjects should be compared in a future study. Third, samples were collected via tonsillar swabs, which may only reflect superficial bacteria.

The strength of this study is that the gut microbiota was

analyzed in the largest number of biopsy-proven IgAN patients. Because there is substantial individual difference in gut microbiota, it is important to collect and analyze enough samples. In addition, this is the first attempt to analyze tonsil and gut microbiota simultaneously in the same population. It could be a start to figure out the crosstalk of microbiota between tonsil and gut. Finally, the important clinical variables at the time of biopsy were collected and the correlation with abundance of microbiota was identified. Therefore, not only key characteristics of the tonsillar and gut microbiota in IgAN, but also the correlations between taxon abundances and clinical features were obtained.

Chapter 3. Conclusion

In conclusion, the microbiota in the tonsils and gut of patients with IgAN differed from those in patients with other kidney diseases and healthy controls. The differential abundance of bacteria could be related to the immune status and pathogenesis of the IgAN. Moreover, new treatment options for IgAN patients, targeting subclinical intestinal inflammation or microbiota modifications are available. Further studies with larger sample sizes and systemic analyses of the gut microbiota and immunological features are necessary to understand the role of the microbiota in IgAN development.

Bibliography

1. D'Amico, G., *The commonest glomerulonephritis in the world: IgA nephropathy.* Q J Med, 1987. **64**(245): p. 709-27.
2. Le, W., et al., *Long-term renal survival and related risk factors in patients with IgA nephropathy: results from a cohort of 1155 cases in a Chinese adult population.* Nephrol Dial Transplant, 2012. **27**(4): p. 1479-85.
3. Lee, H., et al., *Mortality and renal outcome of primary glomerulonephritis in Korea: observation in 1,943 biopsied cases.* Am J Nephrol, 2013. **37**(1): p. 74-83.
4. Barbour, S.J., et al., *Individuals of Pacific Asian origin with IgA nephropathy have an increased risk of progression to end-stage renal disease.* Kidney Int, 2013. **84**(5): p. 1017-24.
5. Kiryluk, K., J. Novak, and A.G. Gharavi, *Pathogenesis of immunoglobulin A nephropathy: recent insight from genetic studies.* Annu Rev Med, 2013. **64**: p. 339-56.
6. Wyatt, R.J. and B.A. Julian, *IgA nephropathy.* N Engl J Med, 2013. **368**(25): p. 2402-14.
7. Floege, J. and J. Feehally, *The mucosa-kidney axis in IgA nephropathy.* Nat Rev Nephrol, 2016. **12**(3): p. 147-56.
8. Suzuki, H., et al., *Toll-like receptor 9 affects severity of IgA nephropathy.* J Am Soc Nephrol, 2008. **19**(12): p. 2384-95.
9. Kiryluk, K., et al., *Discovery of new risk loci for IgA nephropathy implicates genes involved in immunity against intestinal pathogens.* Nat Genet, 2014. **46**(11): p. 1187-96.
10. Wang, T., et al., *Comparison of clinicopathological features between children and adults with IgA nephropathy.* Pediatr Nephrol, 2012. **27**(8): p. 1293-300.
11. Duan, J., et al., *Long-term efficacy of tonsillectomy as a treatment in patients with IgA nephropathy: a meta-analysis.* Int Urol Nephrol, 2017. **49**(1): p. 103-112.
12. Liu, L.L., et al., *Tonsillectomy for IgA nephropathy: a meta-analysis.* Am J Kidney Dis, 2015. **65**(1): p. 80-7.
13. Hotta, O., et al., *Tonsillectomy and steroid pulse therapy significantly impact on clinical remission in patients with IgA nephropathy.* Am J Kidney Dis, 2001. **38**(4): p. 736-43.
14. Xie, Y., et al., *The efficacy of tonsillectomy on long-term renal survival in patients with IgA nephropathy.* Kidney Int, 2003. **63**(5): p. 1861-7.
15. Komatsu, H., et al., *Effect of tonsillectomy plus steroid pulse therapy on clinical remission of IgA nephropathy: a controlled study.* Clin J Am Soc Nephrol, 2008. **3**(5): p. 1301-7.
16. Wang, Y., et al., *A meta-analysis of the clinical remission rate and long-term efficacy of tonsillectomy in patients with IgA nephropathy.* Nephrol Dial Transplant, 2011. **26**(6): p. 1923-31.

17. Suzuki, S., et al., *Haemophilus parainfluenzae antigen and antibody in renal biopsy samples and serum of patients with IgA nephropathy.* Lancet, 1994. **343**(8888): p. 12-6.
18. Suzuki, S., et al., *Synthesis of immunoglobulins against Haemophilus parainfluenzae by tonsillar lymphocytes from patients with IgA nephropathy.* Nephrol Dial Transplant, 2000. **15**(5): p. 619-24.
19. Sharmin, S., et al., *Staphylococcus aureus antigens induce IgA-type glomerulonephritis in Balb/c mice.* J Nephrol, 2004. **17**(4): p. 504-11.
20. Koyama, A., et al., *Staphylococcus aureus cell envelope antigen is a new candidate for the induction of IgA nephropathy.* Kidney Int, 2004. **66**(1): p. 121-32.
21. Watanabe, H., et al., *Comprehensive microbiome analysis of tonsillar crypts in IgA nephropathy.* Nephrol Dial Transplant, 2017. **32**(12): p. 2072-2079.
22. McCarthy, D.D., et al., *Mice overexpressing BAFF develop a commensal flora-dependent, IgA-associated nephropathy.* J Clin Invest, 2011. **121**(10): p. 3991-4002.
23. Coppo, R., *The Gut-Renal Connection in IgA Nephropathy.* Semin Nephrol, 2018. **38**(5): p. 504-512.
24. De Angelis, M., et al., *Microbiota and metabolome associated with immunoglobulin A nephropathy (IgAN).* PLoS One, 2014. **9**(6): p. e99006.
25. Wu, H., et al., *Identification of a novel interplay between intestinal bacteria and metabolites in Chinese patients with IgA nephropathy via integrated microbiome and metabolome approaches.* Ann Transl Med, 2021. **9**(1): p. 32.
26. Sugurmar, A.N.K., et al., *Gut microbiota in Immunoglobulin A Nephropathy: a Malaysian Perspective.* BMC Nephrol, 2021. **22**(1): p. 145.
27. Dong, R., et al., *A Comparative Study of the Gut Microbiota Associated With Immunoglobulin a Nephropathy and Membranous Nephropathy.* Front Cell Infect Microbiol, 2020. **10**: p. 557368.
28. Zhong, Z., et al., *Modifications of gut microbiota are associated with the severity of IgA nephropathy in the Chinese population.* Int Immunopharmacol, 2020. **89**(Pt B): p. 107085.
29. Hu, X., et al., *Fecal microbiota characteristics of Chinese patients with primary IgA nephropathy: a cross-sectional study.* BMC Nephrol, 2020. **21**(1): p. 97.
30. Zhu, A., et al., *Analysis of microbial changes in the tonsillar formalin-fixed paraffin-embedded tissue of Chinese patients with IgA nephropathy.* Pathol Res Pract, 2020. **216**(11): p. 153174.
31. Kang, E., et al., *Biobanking for glomerular diseases: a study design and protocol for KOrea Renal biobank NEtwoRk System TOward NExt-generation analysis (KORNERSTONE).* BMC Nephrol, 2020. **21**(1): p. 367.
32. Levey, A.S., et al., *A new equation to estimate glomerular filtration rate.* Ann Intern Med, 2009. **150**(9): p. 604-12.
33. Park, J.U., et al., *Influence of Microbiota on Diabetic Foot Wound in*

Comparison with Adjacent Normal Skin Based on the Clinical Features. Biomed Res Int, 2019. **2019**: p. 7459236.
34. Lee, J.J., et al., *Analysis of the bacterial microbiome in the small octopus, Octopus variabilis, from South Korea to detect the potential risk of foodborne illness and to improve product management.* Food Res Int, 2017. **102**: p. 51-60.
35. Kim, J.E., et al., *The Association between Gut Microbiota and Uremia of Chronic Kidney Disease.* Microorganisms, 2020. **8**(6).
36. Yoon, S.H., et al., *Introducing EzBioCloud: a taxonomically united database of 16S rRNA gene sequences and whole-genome assemblies.* Int J Syst Evol Microbiol, 2017. **67**(5): p. 1613-1617.
37. Schloss, P.D., et al., *Introducing mothur: open-source, platform-independent, community-supported software for describing and comparing microbial communities.* Appl Environ Microbiol, 2009. **75**(23): p. 7537-41.
38. Zakrzewski, M., et al., *Calypso: a user-friendly web-server for mining and visualizing microbiome-environment interactions.* Bioinformatics, 2017. **33**(5): p. 782-783.
39. Bolyen, E., et al., *Reproducible, interactive, scalable and extensible microbiome data science using QIIME 2.* Nat Biotechnol, 2019. **37**(8): p. 852-857.
40. Callahan, B.J., et al., *DADA2: High-resolution sample inference from Illumina amplicon data.* Nat Methods, 2016. **13**(7): p. 581-3.
41. Douglas, G.M., et al., *PICRUSt2 for prediction of metagenome functions.* Nat Biotechnol, 2020. **38**(6): p. 685-688.
42. Park, J.I., et al., *Comparative analysis of the tonsillar microbiota in IgA nephropathy and other glomerular diseases.* Sci Rep, 2020. **10**(1): p. 16206.
43. Jensen, A., et al., *Molecular mapping to species level of the tonsillar crypt microbiota associated with health and recurrent tonsillitis.* PLoS One, 2013. **8**(2): p. e56418.
44. Nagasawa, Y., et al., *Periodontal disease bacteria specific to tonsil in IgA nephropathy patients predicts the remission by the treatment.* PLoS One, 2014. **9**(1): p. e81636.
45. Johnston, J., et al., *Paired analysis of the microbiota between surface tissue swabs and biopsies from pediatric patients undergoing adenotonsillectomy.* Int J Pediatr Otorhinolaryngol, 2018. **113**: p. 51-57.
46. He, Y., et al., *Regional variation limits applications of healthy gut microbiome reference ranges and disease models.* Nat Med, 2018. **24**(10): p. 1532-1535.
47. Gupta, V.K., S. Paul, and C. Dutta, *Geography, Ethnicity or Subsistence-Specific Variations in Human Microbiome Composition and Diversity.* Front Microbiol, 2017. **8**: p. 1162.
48. Chang, C.L., et al., *Rahnella aquatilis sepsis in an immunocompetent adult.* J Clin Microbiol, 1999. **37**(12): p. 4161-2.
49. Tash, K., *Rahnella aquatilis bacteremia from a suspected urinary source.* J Clin Microbiol, 2005. **43**(5): p. 2526-8.

50. Gaitan, J.I. and M.S. Bronze, *Infection caused by Rahnella aquatilis.* Am J Med Sci, 2010. **339**(6): p. 577-9.
51. Swidsinski, A., et al., *Spatial organisation of microbiota in quiescent adenoiditis and tonsillitis.* J Clin Pathol, 2007. **60**(3): p. 253-60.
52. Dillon, S.M., et al., *Enhancement of HIV-1 infection and intestinal CD4+ T cell depletion ex vivo by gut microbes altered during chronic HIV-1 infection.* Retrovirology, 2016. **13**: p. 5.
53. Ridlon, J.M., et al., *Clostridium scindens: a human gut microbe with a high potential to convert glucocorticoids into androgens.* J Lipid Res, 2013. **54**(9): p. 2437-49.
54. Buffie, C.G., et al., *Precision microbiome reconstitution restores bile acid mediated resistance to Clostridium difficile.* Nature, 2015. **517**(7533): p. 205-8.
55. De Vriese, A.S., et al., *A Proposal for a Serology-Based Approach to Membranous Nephropathy.* J Am Soc Nephrol, 2017. **28**(2): p. 421-430.
56. Kdoqi and F. National Kidney, *KDOQI Clinical Practice Guidelines and Clinical Practice Recommendations for Anemia in Chronic Kidney Disease.* Am J Kidney Dis, 2006. **47**(5 Suppl 3): p. S11-145.
57. Hales, M., K. Solez, and C. Kjellstrand, *The anemia of acute renal failure: association with oliguria and elevated blood urea.* Ren Fail, 1994. **16**(1): p. 125-31.
58. Haller, C., *Hypoalbuminemia in renal failure: pathogenesis and therapeutic considerations.* Kidney Blood Press Res, 2005. **28**(5-6): p. 307-10.
59. Menon, V., et al., *C-reactive protein and albumin as predictors of all-cause and cardiovascular mortality in chronic kidney disease.* Kidney Int, 2005. **68**(2): p. 766-72.
60. Tsuneishi, M., et al., *Composition of the bacterial flora in tonsilloliths.* Microbes Infect, 2006. **8**(9-10): p. 2384-9.
61. Kumar, P.S., et al., *Identification of candidate periodontal pathogens and beneficial species by quantitative 16S clonal analysis.* J Clin Microbiol, 2005. **43**(8): p. 3944-55.
62. Deschamps-Lenhardt, S., et al., *Association between periodontitis and chronic kidney disease: Systematic review and meta-analysis.* Oral Dis, 2019. **25**(2): p. 385-402.
63. Mukherjee, P.K., et al., *Oral mycobiome analysis of HIV-infected patients: identification of Pichia as an antagonist of opportunistic fungi.* PLoS Pathog, 2014. **10**(3): p. e1003996.
64. Ochiai, K., H. Senpuku, and T. Kurita-Ochiai, *Purification of immunosuppressive factor from Capnocytophaga ochracea.* J Med Microbiol, 1998. **47**(12): p. 1087-95.
65. Jansen, H.J., et al., *Degradation of immunoglobulin G by periodontal bacteria.* Oral Microbiol Immunol, 1994. **9**(6): p. 345-51.
66. Liu, X., et al., *Blautia-a new functional genus with potential probiotic properties?* Gut Microbes, 2021. **13**(1): p. 1-21.
67. Rajilic-Stojanovic, M., et al., *Global and deep molecular analysis of microbiota signatures in fecal samples from patients with irritable*

bowel syndrome. Gastroenterology, 2011. **141**(5): p. 1792-801.
68. Nishino, K., et al., *Analysis of endoscopic brush samples identified mucosa-associated dysbiosis in inflammatory bowel disease.* J Gastroenterol, 2018. **53**(1): p. 95-106.
69. Liu, Z., et al., *Self-Balance of Intestinal Flora in Spouses of Patients With Rheumatoid Arthritis.* Front Med (Lausanne), 2020. **7**: p. 538.
70. Zhang, X., et al., *Gut Microbiome and Metabolome Were Altered and Strongly Associated With Platelet Count in Adult Patients With Primary Immune Thrombocytopenia.* Front Microbiol, 2020. **11**: p. 1550.
71. Dei-Cas, I., et al., *Metagenomic analysis of gut microbiota in non-treated plaque psoriasis patients stratified by disease severity: development of a new Psoriasis-Microbiome Index.* Sci Rep, 2020. **10**(1): p. 12754.
72. Tuovinen, E., et al., *Cytokine response of human mononuclear cells induced by intestinal Clostridium species.* Anaerobe, 2013. **19**: p. 70-6.
73. Forbes, J.D., et al., *A comparative study of the gut microbiota in immune-mediated inflammatory diseases-does a common dysbiosis exist?* Microbiome, 2018. **6**(1): p. 221.
74. Park, H.J., et al., *Early-Life Stress Modulates Gut Microbiota and Peripheral and Central Inflammation in a Sex-Dependent Manner.* Int J Mol Sci, 2021. **22**(4).
75. Ten Hagen, K.G., T.A. Fritz, and L.A. Tabak, *All in the family: the UDP-GalNAc:polypeptide N-acetylgalactosaminyltransferases.* Glycobiology, 2003. **13**(1): p. 1R-16R.
76. Zhao, X., et al., *WbpO, a UDP-N-acetyl-D-galactosamine dehydrogenase from Pseudomonas aeruginosa serotype O6.* J Biol Chem, 2000. **275**(43): p. 33252-9.

초록

제목: IgA 신병증에서 편도 및 장내 미생물총의 특징과 임상 양상과의 연관성

배경

최근 연구에서 인간 미생물총의 변화가 숙주의 면역 반응에 중대한 영향을 미친다는 것이 밝혀졌으며, 이는 특히 자가면역질환에서 보고되어 있다. IgA 신병증 환자는 흔히 상기도 감염 또는 위장관 감염과 더불어 육안적 혈뇨를 반복적으로 보인다. 편도와 장에 있는 점막 면역 체계는 IgA 신병증에서 염증의 시작점으로 생각된다. 그러나 IgA 신병증에서의 편도 및 장내 미생물총의 특징은 아직 완전히 밝혀져 있지 않다.

방법

IgA 신병증에서의 편도 및 장내 미생물총의 특징을 알아보기 위해, IgA 신병증과 다른 사구체 질환, 건강인으로 이루어진 3개의 그룹에서 편도와 장내 미생물총을 비교하였다. 편도 미생물총은 총 80개의 편도 스왑 검체를 IgA 신병증 환자 21명, 다른 사구체 질환 36명, 건강인 23명에게서 얻어 분석하였다. 장내 미생물총은 총 194개의 분변 검체를 IgA 신병증 환자 100명, 막성 신장병 36명, 건강인 23명에게서 얻어 분석하였다. 미생물총은 편도 스왑 검체와 분변 검체에서 16S rRNA 유전체를 기반으로 한 Illumina MiSeq system을 사용하여 분석하였다.

Phylogenetic Investigation of Communities by Reconstruction of Unobserved States 2를 이용하여 16S rRNA 유전체 염기서열을 기반으로 기능적 예측을 시행하였다.

결과

IgA 신병증 환자군의 편도 미생물총의 다양성은 다른 사구체 질환군에 비해 높았으나, 건강인 군과 비교했을 때는 차이가 없었다. 주성분 분석에서 IgA 신병증 환자군의 편도 미생물총은 다른 사구체 질환군, 건강인군과 뚜렷한 차이를 보였다. *Rahnella*, *Ruminococcus_g2*, *Clostridium_g21* 속의 비율은 건강인군에 비해 IgA 신병증 환자군에서 유의하게 높았다 (corrected $p < 0.05$), 그 외 몇몇 속의 상대빈도가 예측 사구체여과율, 혈액 요소질소, 혈색소, 알부민과 상관관계를 보였다.
장내 미생물총의 다양성은 세 개의 군에서 차이가 없었다. IgA 신병증 환자군에서 막성 신장병군, 건강인 군에 비해 *Blautia* 속의 상대빈도는 유의하게 높았고, *Sporobacter* 속의 상대빈도는 유의하게 낮았다 (corrected $p < 0.01$). 총 14개의 KEGG Orthology 경로가 면역글로불린 A 신장병 환자군에서 유의한 차이를 보이면서, 해당 군에서 유의하게 확인된 2개의 속과도 연관성이 있는 것으로 확인되었다 (corrected $p < 0.05$).

결론

위의 결과로 미루어, 편도와 장내 미생물총은 IgA 신병증의 임상적 특

징 및 면역학적 발병기전과 관련이 있을 가능성이 있다.